A Critical Review of Data on Field-Scale Dispersion in Aquifers

LYNN W. GELHAR

Department of Civil Engineering, Massachusetts Institute of Technology, Cambridge

CLAIRE WELTY

Department of Civil and Architectural Engineering, Drexel University, Philadelphia, Pennsylvania

KENNETH R. REHFELDT

Illinois State Water Survey, Champaign

A critical review of dispersivity observations from 59 different field sites was developed by compiling extensive tabulations of information on aquifer type, hydraulic properties, flow configuration, type of monitoring network, tracer, method of data interpretation, overall scale of observation and longitudinal, horizontal transverse and vertical transverse dispersivities from original sources. This information was then used to classify the dispersivity data into three reliability classes. Overall, the data indicate a trend of systematic increase of the longitudinal dispersivity with observation scale but the trend is much less clear when the reliability of the data is considered. The longitudinal dispersivities ranged from 10^{-2} to 10^4 m for scales ranging from 10^{-1} to 10^5 m, but the largest scale for high reliability data was only 250 m. When the data are classified according to porous versus fractured media there does not appear to be any significant difference between these aquifer types. At a given scale, the longitudinal dispersivity values are found to range over 2-3 orders of magnitude and the higher reliability data tend to fall in the lower portion of this range. It is not appropriate to represent the longitudinal dispersivity data by a single universal line. The variations in dispersivity reflect the influence of differing degrees of aquifer heterogeneity at different sites. The data on transverse dispersivities are more limited but clearly indicate that vertical transverse dispersivities are typically an order of magnitude smaller than horizontal transverse dispersivities. Reanalyses of data from several of the field sites show that improved interpretations most often lead to smaller dispersivities. Overall, it is concluded that longitudinal dispersivities in the lower part of the indicated range are more likely to be realistic for field applications.

INTRODUCTION

The phenomenon of dispersive mixing of solutes in aquifers has been the subject of considerable research interest over the past 10 years. Characterizing the dispersivity at a particular field site is essential to any effort in predicting the subsurface movement and spreading of a contaminant plume at that location. Both theoretical and experimental investigations have found that field-scale dispersivities are several orders of magnitude greater than lab-scale values for the same material; it is generally agreed that this difference is a reflection of the influence of natural heterogeneities which produce irregular flow patterns at the field scale. Consequently, laboratory measurements of dispersivity cannot be used to predict field values of dispersivity. Instead field-scale tracer tests are sometimes conducted to estimate dispersivity at a particular site.

Early efforts to document the scale dependence of dispersivity [*Lallemand-Barres and Peaudecerf*, 1978; *Anderson*, 1979; *Pickens and Grisak*, 1981; *Beims*, 1983; *Neretnieks*, 1985] were based on field values of dispersivity reported in the literature and the test scales associated with those values. These studies were useful in that they indeed documented field evidence of the scale effect, but they were lacking in that they did not assess the reliability of the data presented. Because we felt that the data would be more meaningful if their variable quality was recognized, we assembled the dispersivity data along with related information from the original sources and evaluated the reliability or quality of these data [*Gelhar et al.*, 1985]. The graphical results of that work have been widely used by both practitioners and theoreticians, often without appropriate consideration of the reliability of the data. For example, recent theoretical developments based on fractal concepts [*Philip*, 1986; *Wheatcraft and Tyler*, 1988; *Neuman*, 1990] have relied on information similar to that in the work by *Gelhar et al.* [1985] but those studies disregarded the issue of the reliability of the data. We feel that it is important to update the dispersivity information including results from recent comprehensive field experiments and at the same time focus on the interpretations of the reliability of the data. With these goals in mind, this work develops the following: (1) an outline of the theoretical description of dispersive mixing in porous media; (2) a tabular summary of existing data on values of field-scale dispersivity and related site information reported in the literature; (3) an evaluation of the reliability or quality of these values based on clearly delineated criteria; and (4) discussion and interpretation of the applied and theoretical implications of the data.

THEORETICAL CONCEPTS OF FIELD-SCALE DISPERSIVE MIXING

The mass balance equation governing the transport of an ideal chemically nonreactive conservative solute by a homo-

geneous fluid (constant density and viscosity) that flows through a rigid saturated porous medium is commonly expressed as [e.g., *Bear*, 1972; *de Marsily*, 1986]

$$\frac{\partial c}{\partial t} + v_i \frac{\partial c}{\partial x_i} = \frac{\partial}{\partial x_i}\left(D_{ij}\frac{\partial c}{\partial x_j}\right) \quad i, j = 1, 2, 3 \quad (1)$$

where c is the solute concentration, v_i is the seepage velocity component in the x_i direction, and D_{ij} are the components of the dispersion coefficient tensor. The right-hand side of (1) represents the net dispersive transport which is presumed to be Fickian, i.e., the dispersive mass flux is proportional to the concentration gradient. Some investigators [e.g., *Robertson and Barraclough*, 1973; *Bredehoeft and Pinder*, 1973] alternatively define the dispersion coefficient tensor including the porosity n as $D_{ij}^* = nD_{ij}$. When it was clear that D_{ij}^* was used in a study, we converted to the more common form used in (1). The mean flow direction is taken to be x_1, with $v_1 = v$, $v_2 = v_3 = 0$. Assuming that x_1, x_2, and x_3 are principal directions, the dispersivity is simply the ratio of the appropriate component of the dispersive coefficient tensor divided by the magnitude of the seepage velocity, v. To distinguish the field-scale dispersivities from laboratory values, the field-scale values are designated by the uppercase letter A [see *Gelhar and Axness*, 1983] and, to allow for anisotropy of transverse dispersion, a third dispersivity coefficient is used as follows:

$$D_{11} = A_L v \qquad D_{22} = A_T v \qquad D_{33} = A_V v \quad (2)$$

where A_L is the longitudinal macrodispersivity (field scale), and A_T is the horizontal transverse macrodispersivity, and A_V is the vertical transverse macrodispersivity.

The classical equation (1) with macrodispersivities (2) is standardly used for applied modeling of field-scale solute transport. The macrodispersivities are considered to be a property of some region of the aquifer. Although the macrodispersivity may be a function of space, in most applications it is assumed constant over a region of the aquifer that encompasses the entire plume both horizontally and vertically. Real solute plumes are observed to be three-dimensional [*LeBlanc*, 1982; *Perlmutter and Lieber*, 1970; *MacFarlane et al.*, 1983] and often of limited vertical extent. Although the classical equation is three-dimensional, the two-dimensional form is most commonly applied. Reasons for the use of the two-dimensional form of the equation include lack of three-dimensional data and in the case of numerical models, restrictions on the size of data arrays in the model. Seldom is the two-dimensional form justified on the basis of site conditions or plume observations.

A number of theoretical studies have proposed methods of describing field-scale dispersive mixing. All of the theories view field-scale dispersion as being produced by some kind of small-scale heterogeneity or variability of the aquifer. At present there is considerable debate concerning how to parameterize the variability and model field-scale solute transport. Assuming a perfectly layered aquifer, one group [*Molz et al.*, 1983, 1986] suggests measuring the variability in detail and modeling the transport in each layer with local-scale dispersivities, thus eliminating the need for a field-scale dispersivity. Again assuming a layered aquifer, a second group suggests the use of a scale-dependent or time-dependent field-scale dispersivity [e.g., *Pickens and Grisak*,

1981; *Dieulin*, 1980]. A third group [e.g., *Gelhar and Axness*, 1983; *Dagan*, 1982; *Neuman et al.*, 1987] has examined more general three-dimensional heterogeneity with stochastic methods and concluded the classical equation with constant field-scale dispersivities is applicable to describe transport over large distances. These stochastic approaches incorporate the effects of practically unknowable small-scale variations in flow by means of macrodispersivities which are used in a deterministic transport model describing the large-scale variations in flow by means of the convection terms. Nonetheless, under what circumstances a field-scale dispersivity can be used to describe field-scale solute transport is still an open question. Until the issue is resolved, the field-scale dispersivity concept can be regarded as a working hypothesis which has a sound theoretical basis and finds wide application.

FIELD DATA ON DISPERSIVITY

Summary of Observations

A literature review was conducted to collect reported values of dispersivity from published analyses of field-scale tracer tests and contaminant transport modeling efforts. The literature sources and pertinent data characterizing each reviewed study are summarized in Table 1 which includes information on 59 different field sites. The information compiled from each study includes site location, description of aquifer material, average aquifer saturated thickness, hydraulic conductivity or transmissivity, effective porosity, mean pore velocity, flow configuration, dimensionality of monitoring network, tracer type and input conditions, length scale of the test or problem, reported values of longitudinal and horizontal and vertical transverse dispersivities, and classification of the reliability of the reported data. Blank entries indicate that the information was not provided in the cited documents. This table summarizes information for purposes of comparison only. More detail regarding a particular study may be found in the original sources.

Aquifer characteristics. As indicated by the second through sixth columns from the left, the study sites represent a wide variety of aquifer conditions and settings. Summarized in these columns is information on aquifer material, saturated thickness, hydraulic conductivity or transmissivity, and velocity. The aquifer thickness for each site is the arithmetic average of the range at that site. Hydraulic conductivity and transmissivity values show the range reported at the site. Reported values for effective porosity vary from 0.5% (for fractured media) to 60% (for porous media). When a value was reported as "porosity," we interpreted this as the effective porosity (interconnected pore space), the value used in analysis of the advection-dispersion equation. Where porosity was reported as "total porosity," we have indicated this in the table. The velocity column indicates the mean pore or seepage velocity at a site. In some cases the values were calculated from information provided on average specific discharge, q, and effective porosity, n, as $v = q/n$. Velocities ranged from 0.0003 to 200 m/d.

Methods of determining dispersivity. The seventh through tenth columns from the left summarize the method used to determine the dispersivity for each site. The seventh, eighth, and ninth columns from the left describe experimental conditions: flow configuration, monitoring, tracer and

input; the tenth column from the left summarizes methods of data interpretation. Dispersivity values were calculated or inferred from one of two types of subsurface solute transport events: large-scale, uncontrolled contamination (naturally occurring or human-induced) events, or controlled tracer tests.

Uncontrolled events are characterized by a source input history that is unknown, transport of contaminants by the ambient flow of groundwater, and solute plumes that often extend over regional scales (hundreds of meters). We describe naturally occurring events as "environmental" tracers, implying chemical constituents associated with uncontrolled natural changes occurring in groundwater before the start of a study. Examples of naturally occurring events include tritium in groundwater from recharge containing atmospheric bomb tritium, seawater intrusion, and mineral dissolution. These events are indicated in the "tracer and input" column by the notation "environmental" along with the type of chemical species reported. Examples of human-induced contamination events include leaks and spills to groundwater from landfills, storage tanks, surface impoundments, and infiltration basins. These types of events are indicated by the notation "contamination" in the tracer and input column. Values of dispersivity for uncontrolled events are commonly determined by fitting a one-, two-, or three-dimensional solute transport model to historical data; i.e., values of dispersivity are altered until model output matches historical solute concentration measurements.

The main features distinguishing controlled tracer tests from uncontrolled ones is that in the former, both the quantity and duration of solute input are known. This is indicated by "step" (continuous input of mass) or "pulse" ("instantaneous" or slug input) in the "tracer and input" column. Controlled tracer tests may be conducted under ambient groundwater flow conditions (also referred to as natural gradient tests), or under conditions where the flow configuration is induced by pumping or recharge. The type of test is reported in the "flow configuration" column. Induced flow configurations include radial, two-well, and forced uniform flow. In radial flow tracer tests, a pulse or step input of tracer is injected at a recharge well and the time distribution of tracer is recorded at an observation well (diverging radial flow test), or the tracer is injected at an observation well and the time distribution is recorded at a distant pumping well (converging radial flow test). In a two-well test, both a recharge well and pumping well are operating; tracer is injected at the recharge well and tracer breakthrough is observed at the pumping well. Recirculation of the water (containing tracer) from the pumping well to the recharge well is often employed. "Forced uniform flow" refers to the flow regime at the Bonnaud site in France, where a uniform flow field was generated between two lines of equally spaced wells, one line recharging and one line pumping, with both screened to the full depth of the aquifer. A discussion of the advantages and disadvantages of different types of tracer tests is presented by *Welty and Gelhar* [1989].

A number of methods have been used to evaluate the data from controlled tracer tests, as indicated by column headed "method of data interpretation." These include fitting of one-, or two- or three-dimensional solute transport analytical solutions, and the method of spatial moments. It should be noted that since the velocity is nonuniform for both radial

and two-well tracer tests, analysis of the data must account for this effect to determine dispersivity properly for such cases. Nonuniform velocity effects have also been observed in ambient flow tracer tests.

The types of tracers used to determine dispersivity at each site are summarized in the "tracer and input" column along with the input conditions. A variety of chemical and microbiological tracers have been employed for controlled tracer tests. Discussions of the suitability of different chemical and microbial species for tracer tests are presented by *Davis et al.* [1980, 1985] and *Betson et al.* [1985]. A primary consideration in designing a controlled tracer test is whether the species is conservative or nonconservative. A conservative tracer is one that moves with the same velocity as the groundwater and does not undergo radioactive decay, adsorption, degradation, chemical reaction (or in the case of microorganisms, death). If any of these effects are present, they must be accounted for in evaluation of the dispersivity. Another factor important in the choice of a tracer is that it is not present in naturally occurring groundwater, or that it is injected at concentrations much higher than natural background levels.

The "monitoring" column indicates whether two- or three-dimensional monitoring was employed at a site. By two-dimensional monitoring we mean depth-averaged (vertically mixed). Three-dimensional monitoring implies point samples with depth. This information is noted because vertical mixing in an observation well influences the concentration of tracer in a water sample. Several studies [*Meyer et al.*, 1981; *Pickens and Grisak*, 1981] have shown that when a tracer is not injected over the full aquifer depth, vertically mixed samples underestimate the tracer concentration and as a result the longitudinal dispersivity is overestimated. This occurs because the tracer occupies only a portion of the vertical thickness. When a sample from the entire thickness is taken, the true tracer concentration is diluted in the well with tracer-free water. If an attempt is made to interpret the diluted ("measured") concentration, the dispersivity will be overestimated. At many sites there was no indication whether point or fully mixed sampling was performed. From examination of the cases where three-dimensional measurements of solute concentrations were made, it is clear that vertical mixing of the tracer as it travels through the aquifer is often very small [*Sudicky et al.*, 1983; *LeBlanc*, 1982; *Freyberg*, 1986; *Garabedian et al.*, 1988, 1991].

Field dispersivities and scale. The "scale of test" column represents the distance traveled from the source for ambient conditions, or the distance between injection and observation wells for the case of an induced flow configuration. The values of dispersivity reported at the indicated scale are given in the second column from the right. Data from the 59 sites yielded 106 values of longitudinal dispersivity, since often multiple investigations or multiple experiments by one investigator were performed at one site. A plot of the longitudinal dispersivity values as a function of scale is presented in Figure 1. The arithmetic average was plotted in cases where a range was reported either for the scale or dispersivity in Table 1. In some cases, values of dispersivity for individual layers were reported as well as an average "aquifer" value. In these cases the latter value was plotted for the given scale. The symbols on Figure 1 indicate whether the dispersivity value is for fractured media (open symbols, 18 values) or porous media (solid symbols, 88

TABLE 1. Summary of

Reference and Site Name	Aquifer Material	Average Aquifer Thickness, m	Hydraulic Conductivity (m/s) or Transmissivity (m²/s)	Effective Porosity, %	Velocity, m/d	Flow Configuration
Adams and Gelhar [1991],§ Columbus, Mississippi	very heterogeneous sand and gravel	8	10^{-5} to 10^{-3} m/s	35	0.03–0.5	ambient
Ahlstrom et al. [1977], Hanford, Washington	glaciofluviatile sands and gravels	64	5.7×10^{-4} to 3.0×10^{-2} m/s			ambient
Bentley and Walter [1983], WIPP	fractured dolomite	5.5		18	0.3	two-well recirculating
Bierschenk [1959] and *Cole* [1972], Hanford, Washington	glaciofluviatile sands and gravels	64	1.7×10^{-1} m²/s	10	26 31	ambinet
Bredehoeft and Pinder [1973], Brunswick, Georgia	limestone	50	6.5×10^{-7} to 8.6×10^{-7} m²/s	35		radial converging
Claasen and Cordes [1975], Amargosa, Nevada	fractured dolomite and limestone	15	5×10^{-2} to 11×10^{-2} m²/s	6–60	0.14–3.4	two-well recirculating
Daniels [1981, 1982], Nevada Test Site	alluvium derived from tuff	500	1.7×10^{-5} m/s		0.04	radial converging
Dieulin [1981], Le Cellier (Lozere, France)	fractured granite	20	3×10^{-4} to 9×10^{-4} m/s	2–8	3	radial converging
Dieulin [1980], Torcy, France	alluvial deposits	6	3×10^{-4} m/s		0.5	ambient
Egboka et al. [1983], Borden	glaciofluvial sand	7–27	10^{-5} to 10^{-7} m/s	38	0.01–0.04	ambient
Fenske [1973], Tatum Salt Dome, Mississippi	limestone	53	4.7×10^{-6} m/s	23	1.2	radial diverging
Freyberg [1986], Borden	glaciofluvial sand	9	7.2×10^{-5} m/s	33 (total)	0.09	ambient
Fried and Ungemach [1971], Rhine aquifer	sand, gravel, and cobbles	12			9.6	radial diverging
Fried [1975], Rhine aquifer (salt mines) southern Alsace, France	alluvial; mixture of sand, gravel, and pebbles with clay lenses	125	10^{-3} m/s			ambient
Fried [1975], Lyons, France (sanitary landfill)	alluvial, with sand and gravel and slightly stratified clay lenses	20			5.0	ambient
Garabedian et al. [1988] Cape Cod, Massachusetts	medium to coarse sand with some gravel overlying silty sand and till	70	1.3×10^{-3} m/s	39	0.43	ambient
Gelhar [1982], Hanford, Washington	brecciated basalt interflow zone					two-well without recirculation
Goblet [1982], site B, France	fractured granite	50	10^{-5} to 10^{-7} m/s		84	radial converging
Grove [1977], NRTS, Idaho	basaltic lava and sediments	76	1.4×10^{-1} to 1.4×10^{1} m²/s	10		ambient
Grove and Beetem [1971], Eddy County (near Carlsbad), New Mexico	fractured dolomite	12		12	3.5	two-well recirculating
Gupta et al. [1975], Sutter Basin, California	sandstone, shale, sand, and alluvial sediments					ambient
Halevy and Nir [1962] and *Lenda and Zuber* [1970], Nahal Oren, Israel	dolomite	100		3.4	4.0	radial converging
Harpaz [1965], southern coastal plain, Israel	sandstone with silt and clay layers	90			14	radial diverging
Helweg and Labadie [1977], Bonsall subbasin, California						ambient
Hoehn [1983], lower Glatt Valley, Switzerland	layered gravel and silty sand	25	9.2×10^{-4} to 6.6×10^{-3} m/s		3.4 1.8 1.2 8.6 4.1 1.7	ambient

Field Observations

Monitoring	Tracer and Input*	Method of Data Interpretation	Scale of Test, m	Dispersivity $A_L/A_T/A_V$,† m	Classification of Reliability of $A_L/A_T/A_V$ (I, II, III)‡
three-dimensional	Br⁻ (pulse)	spatial moments	200	7.5	II
two-dimensional	³H (contamination)	two-dimensional numerical model	20,000	30.5/18.3	III
two-dimensional	PFB, SCN (step)	one-dimensional quasi-uniform flow solution [Grove and Beetem, 1971]	23	5.2	III
two-dimensional	fluorescein (pulse)	one-dimensional uniform flow solution	3,500 4,000	6 460	III III
two-dimensional	Cl⁻ (contamination)	two-dimensional numerical model	2,000	170/52‖	III
two-dimensional	³H (pulse)	one-dimensional quasi-uniform flow solution [Grove and Beetem, 1971]	122	15	III
two-dimensional	³H (contamination)	radial flow type curve [Sauty, 1980]	91	10–30	III
two-dimensional	Cl⁻, I⁻ (pulse)	radial flow type curve [Sauty, 1980]	5	0.5	II
two-dimensional (resistivity)	Cl⁻ (pulse)	one-dimensional uniform flow solution	15	3	III
three-dimensional	³H (environmental)	one-dimensional uniform flow solution	600	30–60	III
	³H (pulse)	one-dimensional uniform flow solution	91	11.6	III
three-dimensional	Br⁻, Cl⁻ (pulse)	spatial moments	90	0.43/0.039	I
	Cl⁻ (pulse)	one-dimensional radial flow numerical model	6	11	III
three-dimensional	Cl⁻ (contamination)	two-dimensional numerical model	800	15/1	III
two-dimensional	EC (contamination)	two-dimensional numerical model	600–1000	12/4	III
three-dimensional	Br⁻ (pulse)	spatial moments	250	0.96/0.018/0.0015	I
two-dimensional	¹³¹I (pulse)	one-dimensional nonuniform flow solution along streamlines [Gelhar, 1982]	17.1	0.60	I
two-dimensional	RhWt, SrCl (pulse)	one-dimensional uniform flow solution including borehole flushing effects	17	2	III
two-dimensional	Cl⁻ (contamination)	two-dimensional numerical model	20,000	91/91	III
two-dimensional	³H (step)	one-dimensional quasi-uniform flow solution [Grove and Beetem, 1971]	55	38.1	III
	Cl⁻ (environmental)	three-dimensional numerical model	50,000	80–200/ 8–20	III
two-dimensional	⁶⁰Co (pulse)	one-dimensional uniform flow solution	250	6	II
two-dimensional	Cl⁻ (step)	one-dimensional radial flow solution	28	0.1–1.0	II
	TDS (contamination)	two-dimensional numerical model	14,000	30.5/9.1	III
two-dimensional	uranine (pulse)	one-dimensional uniform flow solution for layers	4.4 4.4 4.4 10.4 10.4 10.4	0.1 0.01 0.2 0.3 0.04 0.7	III III

TABLE 1.

Reference and Site Name	Aquifer Material	Average Aquifer Thickness, m	Hydraulic Conductivity (m/s) or Transmissivity (m^2/s)	Effective Porosity, %	Velocity, m/d	Flow Configuration
Hoehn and Santschi [1987], lower Glatt Valley, Switzerland	layered gravel and silty sand	27.5	8.1×10^{-5} to 6.6 $\times 10^{-3}$ m/s		1.5 3.2 5.6 3.9 3.2	ambient ambient
Huyakorn et al. [1986], Mobile, Alabama	layered medium sand	21.6		0.35		two-well without recirculation
Iris [1980], Campuget (Gard), France	alluvial deposits	9	3.6×10^{-3} m^2/s		0.05	radial diverging
Ivanovitch and Smith [1978], Dorset, England	fractured chalk		2.2×10^{-3} m/s (fast pulse)	0.5	57.6	radial converging
	chalk		3.6×10^{-4} m/s (slow pulse)	2.3	9.6	radial converging
Kies [1981], New Mexico State University, Las Cruces	fluvial sands		9.55×10^{-5} m/s	42 (total)		ambient
Klotz et al. [1980], Dormach, Germany	fluvioglacial gravels	14			20	radial converging
Konikow [1976], Rocky Mountain Arsenal	alluvium			30		ambient
Konikow and Bredehoeft [1974], Arkansas River valley (at La Junta, Colorado)	alluvium, inhomogeneous clay, silt, sand and gravel		2.4×10^{-4} to 4.2 $\times 10^{-3}$ m/s	20		ambient
Kreft et al. [1974], Poland	sand	2.5	3.1×10^{-5} to 1.5×10^{-4} m/s; 1.2 $\times 10^{-4}$ m^2/s	24	29	radial converging
Kreft et al. [1974], Zn-Pb deposits, Poland	fractured dolomite	57	2.5×10^{-4} to 4.7×10^{-4} m/s	2.4	7.5 100	radial converging
	fractured dolomite	48	2.5×10^{-4} to 4.7×10^{-4} m/s	2.4	60.1 22.7	radial converging
Kreft et al. [1974], sulfur deposits, Poland	limestone	7	1.1×10^{-4} m/s	12.3	10 10.8	radial converging
	limestone	7	1.1×10^{-4} m/s	12.3	8.6	radial converging
Lau et al. [1957], University of California, Berkeley	sand and gravel with clay lenses	1.5	9×10^{-4} m/s	30	7	radial diverging
Lee et al. [1980], Perch Lake, Ontario, (lake bed)	sand		3.2×10^{-5} m/s		0.14	ambient
Leland and Hillel [1981], Amherst, Massachusetts	fine sand and glacial till	0.75	2.4 to 3×10^{-5} m/s	40	0.3–0.6	ambient
Mercado [1966], Yavne region, Israel	sand and sandstone with some silt and clay	80	2.1×10^{-8} to 2.4×10^{-8} m^2/s	23.3	0.84–3.4	radial diverging/converging
Meyer et al. [1981]; Koeberg Nuclear Power Station, South Africa	sand	20			0.12	ambient
Molinari and Peaudecerf [1977] and *Sauty* [1977], Bonnaud, France	sand	3	8.3×10^{-4} to 1.1×10^{-3} m^2/s		2.7 1.0 2.4 1.0 2.0 2.0	forced uniform
Moltyaner and Killey [1988a, b], Twin Lake aquifer (Chalk River)	fluvial sand			40.8 (total)	1.2	ambient
Naymik and Barcelona [1981], Meredosia, Illinois (Morgan County)	unconsolidated sand and gravel	27	2.2×10^{-2} to 4.3×10^{-2} m^2/s			ambient

(continued)

Monitoring	Tracer and Input*	Method of Data Interpretation	Scale of Test, m	Dispersivity $A_L/A_T/A_V$,† m	Classification of Reliability of $A_L/A_T/A_V$ (I, II, III)‡
two-dimensional	uranine (pulse)	temporal moments	4.4	1.1	II
two-dimensional	^{3}H (environmental)	temporal moments	10.4	1.2	II
			100	6.7	III
			110	10.0	III
			500	58.0	III
two-dimensional	Br⁻ (pulse)	two-dimensional numerical model	38.3	4.0	I
three-dimensional	heat (pulse)	two-dimensional radial numerical model	40	3/1.5	II
	^{82}Br (pulse)	one-dimensional uniform flow solution	8	3.1	III
	^{82}Br (pulse)	one-dimensional uniform flow solution	8	1.0	III
two-dimensional	NO₃⁻ (pulse)	two-dimensional uniform flow solution	25	1.6/0.76	III
two-dimensional	^{82}Br, uranine (pulse)	one-dimensional uniform flow solution	10	5, 1.9	II
	Cl⁻ (contamination)	two-dimensional numerical model	13,000	30.5	III
two-dimensional	dissolved solids (contamination)	two-dimensional numerical model	18,000	30.5/9.1	III
two-dimensional	^{131}I (pulse)	one-dimensional uniform flow solution	5–6	0.18	II
	^{131}I (pulse)	one-dimensional uniform flow solution	22	44–110	II
	^{131}I (pulse)	one-dimensional uniform flow solution	21.3	2.1	II
	^{58}Co (pulse)	one-dimensional uniform flow solution	27	2.7–27	II
	^{58}Co (pulse)	one-dimensional uniform flow solution	41.5	20.8	II
	Cl⁻ (step)	one-dimensional radial numerical model	19	2–3	I
three-dimensional	Cl⁻ (pulse)	one-dimensional uniform flow solution	≤6	0.012	II
three-dimensional	Cl⁻ (pulse)	two-dimensional uniform flow solution	4	0.05–0.07	III
three-dimensional	^{60}Co, Cl⁻ (step)	one-dimensional radial flow solution	≤115 (observation wells)	0.5–1.5 (injection phase)	I
three-dimensional	^{131}I (pulse)	one-dimensional uniform flow solution for layers	2–8	0.01, 0.03, 0.01, 0.05 for layers; 0.42 for depth average	III
two-dimensional	I⁻	two-dimensional uniform flow solution	13	0.79	I
	^{3}H		13	1.27	I
	^{131}I		13	0.72	I
	^{131}I		26	2.23	I
	^{131}I		33.2	1.94/0.11	I
	^{131}I (pulse)		32.5	2.73/0.11	I
three-dimensional	^{131}I (pulse)	two-dimensional uniform flow solution	40	0.06–0.16/···/ 0.0006–0.002	II
two-dimensional	NH₃ (contamination)	two-dimensional numerical model	16.4	2.13–3.35/ 0.61–0.915	III

TABLE 1.

Reference and Site Name	Aquifer Material	Average Aquifer Thickness, m	Hydraulic Conductivity (m/s) or Transmissivity (m²/s)	Effective Porosity, %	Velocity, m/d	Flow Configuration
New Zealand Ministry of Works and Development [1977] Heretaunga aquifer, New Zealand: Roys Hill site	gravel with cobbles	100	0.29 m²/s	22	150–200	ambient
Flaxmere site 2	alluvium (gravels)	120	0.37 m²/s	22	20–25	ambient
Hastings City rubbish dump	alluvium (gravels)		$0.14, 0.35$ m²/s	20		ambient
Oakes and Edworthy [1977], Clipstone, United Kingdom	sandstone	44	2.4×10^{-6} to 1.4×10^{-4} m/s	32–48	5.6, 4.0 9.6	radial diverging
					2.4, 3.6	radial converging
Papadopulos and Larson [1978], Mobile, Alabama	medium to fine sand interspersed with clay and silt	21	5×10^{-4} m/s (horizontal) and 5.1×10^{-5} m/s (vertical)	25	0.05	radial diverging
Pickens and Grisak [1981], Chalk River	sand	8.5	2×10^{-5} to 2×10^{-4} m/s	38	0.15	two-well recirculating
	sand	8.5	2×10^{-5} to 2×10^{-4} m/s	38	0.15	radial diverging/converging
Pinder [1973], Long Island	glacial outwash	43	7.5×10^{-4} m/s	35	0.43	regional
Rabinowitz and Gross [1972], Roswell Basin, New Mexico	fractured limestone	61	1.1×10^{-2} to 2.9×10^{-1} m²/s	1	11–21	regional
Rajaram and Gelhar [1991], Borden	glaciofluvial sand	9	7.2×10^{-5} m/s	33 (total)	0.09	ambient
Roberts et al. [1981], Palo Alto bay lands	sand, gravel, and silt	2	1.25×10^{-3} m²/s (lower aquifer); 5.0×10^{-4} m²/s (upper aquifer)	25	15.5 12.0 3.5 25.6 7.9	radial diverging
Robertson [1974] and *Robertson and Barraclough* [1973], NRTS, Idaho	basaltic lava and sediments	76	1.4×10^{-1} to 1.4×10^{1} m²/s	10	1.5–8	regional
Robson [1974, 1978], Barstow, California	alluvial sediments	27	2.1×10^{-4} to 1×10^{-2} m²/s	40		two-well recirculating
				40	3	regional
Robson [1978], Barstow, California	alluvial sediments	30.5	5×10^{-4} m/s	40		regional
Rousselot et al. [1977], Byles–Saint Vulbas near Lyon, France	clay, sand, and gravel	12	6.5×10^{-3} to 1.5×10^{-2} m/s	14 2.1–18 1.8–5.9 11–24	18 11.5, 3.8 46.7, 16 24	radial converging
Sauty [1977], Corbas, France	sand and gravel	12			125, 100 15.5, 78 6.9	radial converging
Sauty et al. [1978], Bonnaud, France	sand	3	8.3×10^{-4} to 1.1×10^{-3} m²/s			radial diverging
Segol and Pinder [1976], Cutler area, Biscayne Bay aquifer, Florida	fractured limestone and calcareous sandstone	30.5	0.45×10^{-2} m/s (horizontal) and 0.09×10^{-4} m/s (vertical)	25	20	ambient
Sudicky et al. [1983], Borden	glaciofluvial sand	7–27	4.8×10^{-5} to 7.6×10^{-5} m/s	38	0.07– 0.25	ambient
Sykes et al. [1982, 1983], Borden	sand		5.8 to 7.2×10^{-5} m/s	35		ambient
Sykes et al. [1983], Mobile, Alabama	sand, silt, and clay	21	5×10^{-4} m/s (horizontal) and 2.5×10^{-5} m/s (vertical)	25	0.05	radial diverging

(continued)

Monitoring	Tracer and Input*	Method of Data Interpretation	Scale of Test, m	Dispersivity $A_L/A_T/A_V$,† m	Classification of Reliability of $A_L/A_T/A_V$ (I, II, III)‡
three-dimensional	^{131}I, RhWt, ^{82}Br, Cl$^-$, E. Coli (pulse)	three-dimensional uniform flow solution	54–59	1.4–11.5/ 0.1–3.3/ 0.04–0.10	II
three-dimensional	RhWt, ^{82}Br (pulse)	three-dimensional uniform flow solution	25	0.3–1.5/ ··/0.06	II
three-dimensional	Cl$^-$ (contamination)	three-dimensional uniform flow solution	290	41/10/0.07	III
two-dimensional	^{82}Br (pulse)	radial flow numerical model	6	0.16, 0.38	II
			3	0.31	II
two-dimensional	Cl$^-$, I$^-$ (pulse)		6	0.6	II
			3	0.6	II
two-dimensional	heat (step)	two-dimensional numerical model	57.3	1.5	II
three-dimensional	^{51}Cr (step)	one-dimensional quasi-uniform flow solution	8	0.5	III
three-dimensional	^{131}I (step)	one-dimensional radial flow solution	3	0.03	III
three-dimensional	Cr^{+6} (contamination)	two-dimensional numerical model	1,000	21.3/4.2	III
two-dimensional	^{3}H (environmental)	one-dimensional uniform flow solution	32,000	20–23	III
three-dimensional	Br$^-$, Cl$^-$ (pulse)	spatial moments	90	0.50/0.05/ 0.0022	I
two-dimensional	Cl$^-$ (step)	one-dimensional uniform flow solution	11	5	III
			20	2	III
			40	8	III
			16	4	III
			43	11	III
two-dimensional	Cl$^-$ (contamination)	two-dimensional numerical model	20,000	910/1370‖	III
two-dimensional	Cl$^-$ (step)	one-dimensional quasi-uniform flow solution	6.4	15.2	III
two-dimensional	TDS (contamination)	two-dimensional numerical model	10,000	61/18	III
three-dimensional	TDS (contamination)	two-dimensional numerical model (vertical section)	3,200	61/··/0.2	III
two-dimensional	I$^-$ (pulse)	one-dimensional uniform flow solution for layers	9.3	6.9	II
			5.3	0.3, 0.7	III
			10.7	0.46, 1.1	III
			7.1	0.37	II
two-dimensional	I$^-$ (pulse)	one-dimensional uniform flow solution for layers	25	11, 1.25	III
			50	25, 6.25	III
			150	12.5	II
two-dimensional	heat (step)	one-dimensional radial flow solution	13	1.0	II
three-dimensional	Cl$^-$ (environmental)	two-dimensional numerical model	490	6.7/··/0.67	III
three-dimensional	Cl$^-$ (pulse)	three-dimensional uniform flow solution	11	0.08/0.03	II
			0.75	0.01/0.005	II
three-dimensional	Cl$^-$ (pulse)	two-dimensional numerical model	700	7.6/··/0.31	III
three-dimensional	heat (step)	three-dimensional numerical model	57.3	0.76/··/0.15	II

TABLE 1.

Reference and Site Name	Aquifer Material	Average Aquifer Thickness, m	Hydraulic Conductivity (m/s) or Transmissivity (m²/s)	Effective Porosity, %	Velocity, m/d	Flow Configuration
Vaccaro and Bolke [1983], Spokane aquifer, Washington and Idaho	glaciofluvial sand and gravel	152	9×10^{-5} m²/s to 6.5 m²/s	7–40	0.003–2.8	ambient
Valocchi et al. [1981], Palo Alto bay lands	sand, gravel, and silt	2	1.25×10^{-3} m²/s (lower aquifer); 5.0×10^{-4} m²/s (upper aquifer)	25	27	radial diverging
Walter [1983], WIPP	fractured dolomite	7	8.0×10^{-5} m²/s	0.7 and 11 (along separate paths)	4.7, 2.4	radial converging
Webster et al. [1970], Savannah River Plant, South Carolina	crystalline, fractured schist and gneiss	76	3.6×10^{-7} m/s		1.3 21.4	two-well recirculating
Werner et al. [1983], Hydrothermal Test Site, Aefligen, Switzerland	gravel	20	6×10^{-3} m/s	17	9.1	ambient
Wiebenga et al. [1967] and *Lenda and Zuber* [1970], Burdekin Delta, Australia	sand and gravel	6.1	5.5×10^{-3} m/s	32	29	radial converging
Wilson [1971] and *Robson* [1974], Tucson, Arizona	unconsolidated gravel, sand, and silt		5.75×10^{-3} m²/s	38		two-well without recirculation radial diverging
Wood [1981], Aquia Formation, southern Maryland	sand	1,000	2.9×10^{-4} to 8.7×10^{-4} m²/s	35	0.0003– 0.0007	ambient
Wood and Ehrlich [1978] and *Bassett et al.* [1980], Lubbock, Texas	sand and gravel	17	3.2×10^{-3} to 4.4×10^{-3} m²/s		78	radial converging

*TDS denotes total dissolved solids; EC, electrical conductivity; PFB, pentafluorobenzoate; MTFMB, metatrifluoromethylbenzoate; MFB, metafluorobenzoate; Para-FB, parafluorobenzoate; RhWT, rhodamine-WT dye; and SCN, thiocyanate.

†A_L denotes longitudinal dispersivity; A_T, horizontal transverse dispersivity; and A_V, vertical transverse dispersivity. Reported values for A_L, A_T, and A_V are separated by slashes. Absence of slashes means that values were reported for A_L only. A comma or a dash separating entries means that multiple values or a range of values, respectively, were reported for a particular dispersivity component.

‡For description of classification criteria, see text.

§E. E. Adams and L. W. Gelhar, Field study of dispersion in a heterogeneous aquifer: Spatial moments analysis (submitted to *Water Resources Research*, 1991).

‖Porosity-corrected dispersivity value.

values). The type of event evaluated is indicated by a circle (tracer test, 83 values), triangle (contamination event, 15 values), or square (environmental tracer, eight values). The total numbers of values of dispersivity for each type of medium and test are shown in Table 2. Any reported values of horizontal transverse dispersivity or vertical transverse dispersivity are also listed in the dispersivity column of Table 1. For the cases examined, 24 values of horizontal transverse dispersivity and nine values of vertical transverse dispersivity were reported. In nearly all cases, the horizontal values were found to be 1–2 orders of magnitude less than the longitudinal values, and the vertical values smaller by another order of magnitude.

Evaluation of Dispersivity Data

From Figure 1, it appears that longitudinal dispersivity increases with scale. Field observations of dispersivity ranged from 0.01 m to approximately 5500 m at scales of 0.75 m to 100 km. The longitudinal dispersivity for the two types of aquifer material (porous versus fractured media) tends to

scatter over a similar range, although at a smaller scale fractured media seem to show higher values. At each scale there is at least a two-order-of-magnitude range in dispersivity. Because we noted a number of problems with data and their interpretation as we gathered them for Table 1, we would regard any conclusions about Figure 1 with skepticism until further qualifying statements can be made about the data points. Typical problems that we found with the studies reported in Table 1 include the following: data analysis not matched to flow configuration; mass input history unknown; nonconservative effects of tracer not accounted for; dimensionality of the monitoring not matched to the dimensionality of the analysis; and assumption of distinct geologic layers in analysis when their actual presence was not documented. Based on these problems, we decided to rate the data as high (I), medium (II), or low (III) reliability according to the criteria set forth below. Table 3 lists the criteria used to designate either high- or low-reliability data. No specific criteria were defined for the intermediate classification; it encompasses the dispersivity

(continued)

Monitoring	Tracer and Input*	Method of Data Interpretation	Scale of Test, m	Dispersivity $A_L/A_T/A_V$,† m	Classification of Reliability of $A_L/A_T/A_V$ (I, II, III)‡
	Cl^- (contamination)	two-dimensional numerical model	43,400	91.4/27.4	III
	Cl^- (step)	two-dimensional numerical model	16	1.0/0.1	I
two-dimensional	MTFMB, PFB, MFB, para-FB (pulse)	one-dimensional uniform flow solution	30	10–15	III
two-dimensional	^{85}Sr ^{85}Br (pulse)	one-dimensional quasi-uniform flow solution	538	134	III
three-dimensional	heat (step)	one-dimensional numerical model	700 37 105 200	130–234 131 208 234	III III III III
	^{131}I, ^{3}H (pulse)	one-dimensional uniform flow solution	18.3	0.26	II
three-dimensional	Cl^- (step)	one-dimensional quasi-uniform flow solution	79.2	15.2	III
two-dimensional	Cl^- (step)	one-dimensional radial flow solution	4.6	0.55	III
	Na^+ (environmental)	one-dimensional uniform flow solution	10^5	5,600–40,000	III
two-dimensional	I^- (pulse)	one-dimensional radial flow solution	1.52	0.015	II

values that do not fall into the high or low groups. These classifications do not place strict numerical confidence limits on reported dispersivities, but rather are intended to provide an order-of-magnitude estimate of the confidence we place on a given value. In general, we consider high-reliability dispersivity values to be accurate within a factor of 2. Low-reliability values are considered to be no more accurate than within 1 or 2 orders of magnitude. Intermediate reliability falls somewhere between the extremes. We wish to make a distinction between the judgment of the reliability of the reported dispersivity and the worth of a study. Often, the purpose of a study was for something other than the determination of dispersivity. Our classification of dispersivity is not intended as a judgment on the quality of a study as a whole, but rather to provide us with some criteria with which to screen the large number of data values obtained. By then examining the more reliable data, conclusions which evolve from the data will be more soundly based and alternative interpretations may become apparent.

High-reliability dispersivity data. For a reported dispersivity value to be classified as high reliability, each of the following criteria must have been met.

1. The tracer test was either ambient flow with known input, diverging radial flow, or a two-well pulse test (without recirculation). These three test configurations produce breakthrough curves which are sensitive to the dispersion coefficient and appear to work well in field applications [*Welty and Gelhar*, 1989]. The radial converging flow test is generally considered less satisfactory than the diverging test because breakthrough curves at the pumping well for the converging test frequently exhibit tailing, which complicates the interpretation of these tests. Some researchers attribute this behavior to two or more discrete geologic layers and try to reproduce the observed breakthrough curve by superposition of breakthrough curves in each layer, where the properties of each layer may differ [e.g., *Ivanovitch and Smith*, 1978; *Sauty*, 1977]. The problem with this interpretation is that there are typically numerous heterogeneities on a small scale that cannot be attributed solely to identifiable layers. One possible explanation of the tailing in radial convergent tests is sometimes termed "borehole flushing," where the tail of the breakthrough curve is attributed to the slow flushing of the input slug of tracer out of the injection borehole by the ambient groundwater flow. *Goblet* [1982] measured the slow flushing of tracer out of the
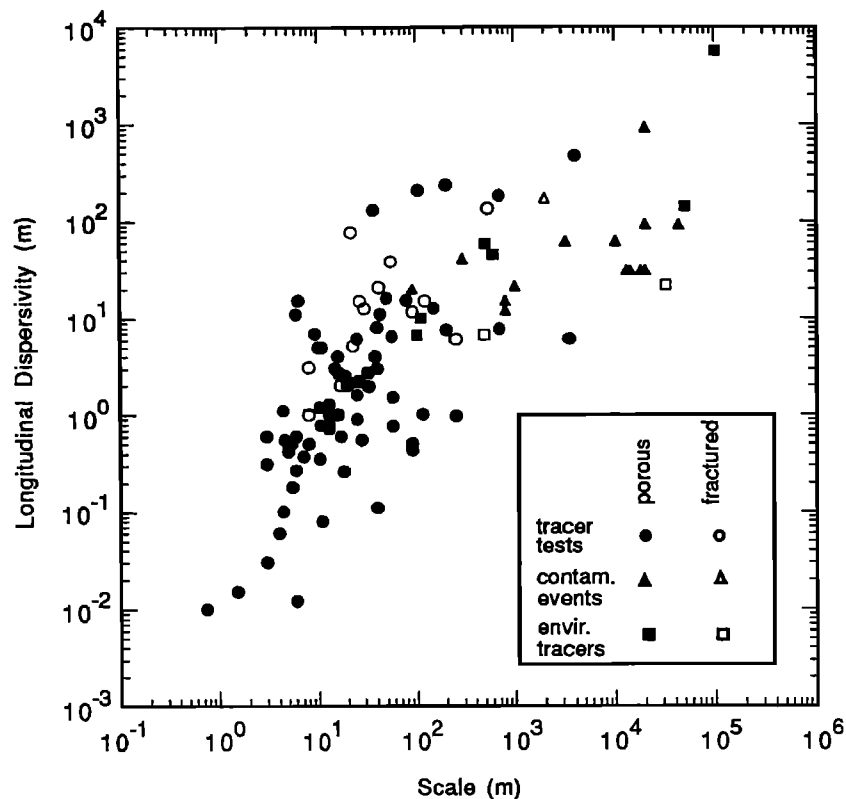
Fig. 1. Longitudinal dispersivity versus scale of observation identified by type of observation and type of aquifer. The data are from 59 field sites characterized by widely differing geologic materials.

borehole and modeled the effect as an exponentially decreasing input. His solution reproduced the tailing observed at the pumping well. In cases where borehole flushing was observed and accounted for, dispersivities obtained from a radial convergent flow test were not excluded from the high-reliability category.

2. The tracer input must be well defined. Both the input concentration and the temporal distribution of the input concentrations must be known (measured). If not, the input is another unknown in the solution of the advection-dispersion equation, and we are less confident in the resulting value of dispersivity.

3. The tracer must be conservative. A reactive or nonconservative tracer complicates the governing equations and resulted in additional parameters that must be estimated. Consequently, we are less confident in the resulting dispersivity. Tracers such as Cl^-, I^-, Br^-, and tritium were considered to be conservative.

4. The dimensionality of the tracer concentration measurements was appropriate. A tracer introduced into an aquifer will spread in three spatial dimensions. High-reliability dispersivities were judged to be those where three-dimensional monitoring was used in all cases except where the aquifer tracer had been injected and measured over the full depth of the aquifer; in this case two-dimensional monitoring was acceptable. In all other cases, where the dimension of the measurement was either not reported or where two-dimensional measurements were used where three-dimensional measurements should have been used, the dispersivity values were judged to be of lower reliability.

5. The analysis of the concentration data was appropriate. Since the interpretation of the tracer data is necessarily linked to the type of tracer test to which the interpretation method is applied, these two features of the field studies were evaluated together. The three general categories of data interpretation can be grouped as follows: (1) breakthrough curve analysis, usually applied to uniform ambient flow tests and radial flow tests [e.g., *Sauty*, 1980]; (2) method of spatial moments, applied to uniform ambient flow tests [*Freyberg*, 1986]; and (3) numerical methods, applied to contamination events [e.g., *Pinder*, 1973; *Konikow and Bredehoeft*, 1974].

A common difficulty with the interpretation of concentration data using breakthrough curve matching to determine dispersivity is the assumption that the dispersivity is constant. The field data assembled in this review suggest that this assumption is not valid, at least for small-scale tests (tens of meters). At larger scales (hundreds of meters) an asymptotic constant value of dispersivity is predicted by some theories. However, at most sites the displacement distance after which the dispersivity is constant is not

TABLE 2. Numbers of Dispersivities for Different Types of Tests and Media

Media Type	Tracer Type			
	Artificial	Contamination	Environmental	Total
Porous	68	14	6	88
Fractured	15	1	2	18
Total	83	15	8	106

TABLE 3. Criteria Used to Classify the Reliability of the
Reported Dispersivity Values

Classification	Criteria
High reliability	Tracer test was either ambient flow, radial diverging flow, or two-well instantaneous pulse test (without recirculation). Tracer input was well defined. Tracer was conservative. Spatial dimensionality of the tracer concentration measurements was appropriate. Analysis of the tracer concentration data was appropriate.
Low reliability	Two-well recirculating test with step input was used. Single-well injection-withdrawal test with tracer monitoring at the single well was used. Tracer input was not clearly defined. Tracer breakthrough curve was assumed to be the superposition of breakthrough curves in separate layers. Measurement of tracer concentration in space was inadequate. Equation used to obtain dispersivity was not appropriate for the data collected.

known. Data for which no a priori assumptions were made regarding the dispersivity were considered to be highly reliable.

A second major problem with many of the analyses reviewed was that a one- or two-dimensional solution to the advection-dispersion equation was used when the spreading of the plume under consideration was three-dimensional in nature. High-reliability dispersivities were those for which the dimensionality of the solute plume, the solute measurements, and the data analyses were consistent.

Low-reliability dispersivity data. A reported dispersivity was classified as being of low reliability if one of the following criteria was met.

1. The two-well recirculating test with a step input was used. The problem with this configuration is that, except for very early time where concentrations are low, the breakthrough curve is not strongly influenced by dispersion, but rather is determined by the different travel times along the flow paths established by injection and pumping wells [*Welty and Gelhar*, 1989]. As a result, the two-well test with a step input is generally insensitive to dispersion. For this reason all tests of this type were considered to produce data of low reliability.

2. The single-well injection-withdrawal test was used with tracer monitoring at the pumping well. A difficulty encountered in the small-scale, single-well, injection-withdrawal test (where water is pumped into and out of one well) is that if observations are made at the production well, the dispersion process observed is different from one of unidirectional flow. The problem stems from the fact that macrodispersion near the injection well is due to velocity differences associated with layered heterogeneity of the hydraulic conductivity. In the single-well test with observations made at the production well, the effect observed is that of reversing the velocity of the water. If the tracer travels at different velocities in layers as it radiates outward, it will also travel with the same velocity pattern as it is drawn back

to the production well. As a result, the mixing process is partially reversible and the dispersivity would be underestimated relative to the value for unidirectional flow. *Heller* [1972] has carried out experiments which demonstrate the reversibility effect on a laboratory scale.

3. The tracer input was not clearly defined. When a contamination event or environmental tracer is modeled, the tracer input (both quantity and temporal distribution) is not well defined and becomes another unknown in solving the advection-dispersion equation.

4. The tracer breakthrough curve was assumed to be the superposition of breakthrough curves in separate layers when there was little or no evidence of such layers at the field site. These studies generally assume that the porous medium is perfectly stratified, which, especially at the field scale, may not be a valid assumption. At a small scale (a few meters) where the existence of continuous layers may be a reasonable assumption, the dispersivity of each layer does not represent the field-scale parameter. The field-scale dispersivity is a result of the spreading due to the different velocities in each layer.

5. The measurement of tracer concentration in space was inadequate. Under ambient flow conditions the tracer is usually distributed in three-dimensional space, but if the measurements are two-dimensional then the actual tracer cloud cannot be analyzed lacking the appropriate data. If the tracer is introduced over the entire saturated thickness, then two-dimensional measurements would be adequate.

6. The equation used to obtain dispersivity was not appropriate for the data collected. Various assumptions regarding flow and solute characteristics are made in obtaining a solution to the advection-dispersion equation. To apply a particular solution to the data from a field experiment, the assumptions in that solution must be consistent with the experimental conditions. One common example is the case of applying a one-dimensional (uniform velocity) flow solution to a radial flow test in which the converging (or diverging) flow field around the pumping or injection well is clearly nonuniform.

Results of classification. From the classification process, 14 dispersivity values were judged to be of high reliability. The sites where these values were determined include Borden, Ontario, Canada; Otis Air Force Base, Cape Cod, Massachusetts; Hanford, Washington; Mobile, Alabama; University of California, Berkeley; Yavne region, Israel; Bonnaud, France (six tests); and Palo Alto bay lands. There were 61 values judged to be of low reliability for one or more of the reasons discussed above; 31 sites provided data judged to be of intermediate value. Figure 2 depicts the longitudinal dispersivity data replotted with symbols reflecting the reliability classification; the largest symbols indicate data judged to be of highest reliability.

The general compilation of all dispersivity data in Figure 1 indicates that dispersivity might increase indefinitely with scale, but after critically evaluating the data in terms of reliability as shown in Figure 2, it is evident that this trend cannot be extrapolated with confidence to all scales. The largest high-reliability dispersivity value is 4 m (Mobile, Alabama) and the largest scale of high-reliability values is 250 m (Cape Cod, Massachusetts). It is not clear from these data whether dispersivity increases indefinitely with scale or whether the relationship becomes constant for very large scales, as would be predicted by some theories. This points
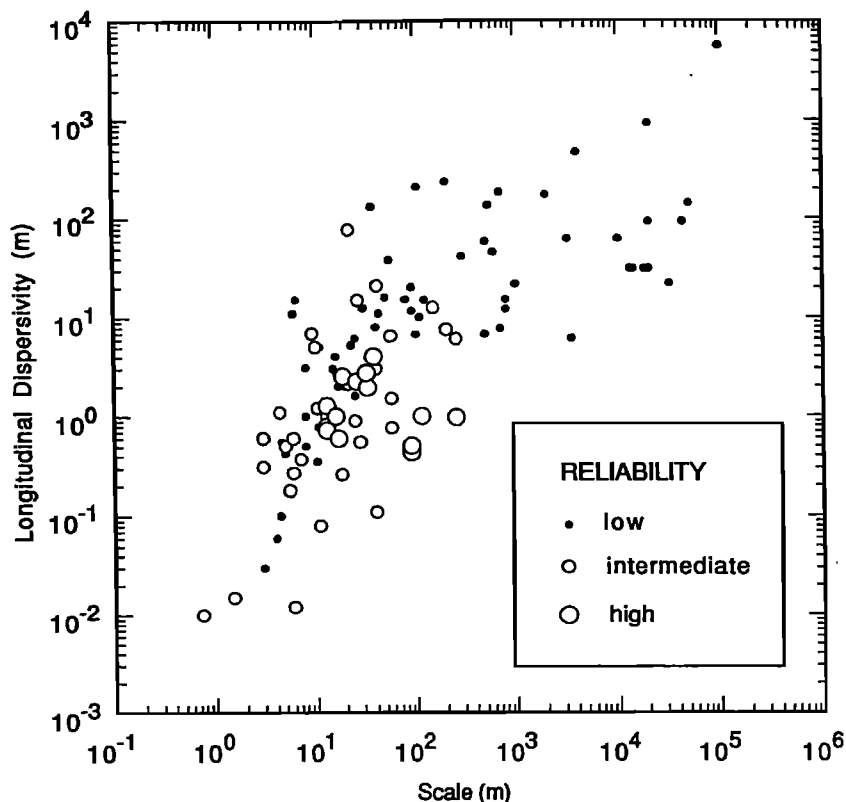
Fig. 2.   Longitudinal dispersivity versus scale with data classified by reliability.

to a need for reliable data at scales larger than 250 m. Whether conducting controlled tracer tests at these very large scales is feasible is open to question.

When the reliability of the data is considered, the apparent difference between fractured and porous media at small scales (Figure 1) is regarded to be less significant because none of the fractured media data are of high reliability.

Reanalyses of Selected Dispersivity Data

In cases where the concentration data collected were of high reliability but the method of analysis could be improved, we reevaluated the data to determine a dispersivity value which we judged to be of higher reliability. The details of these analyses are reported by Welty and Gelhar [1989]. The results are summarized here.

Corbas, France.   The data from this converging radial flow tracer test are reported by Sauty [1977]. These data are of particular interest because tests were conducted at three different scales in the same aquifer material; tracer was injected at 25, 50, and 150 m from a pumping well. Sauty [1977] evaluated these data using uniform flow solutions to the one-dimensional advection-dispersion equation. At the two smaller-scale tests, he assumed a two-layer scheme, although this assumption was not supported by geologic evidence. For this reason the data at the smaller scales were rated to be of lower reliability than the data at 150 m. We reevaluated these data using a solution that accounts for nonuniform, convergent radial flow effects and that makes no assumptions about geologic layers [Welty and Gelhar, 1989]. The values of dispersivity reported by Sauty at 25 m are 11 m and 1.25 m for the two hypothesized layers; we calculated

a value of 2.4 m without the assumption of layers. At 50 m, Sauty calculated dispersivity values of 25 m and 6.25 m for the two layers; we calculate an overall value of 4.6 m. At a scale of 150 m, Sauty calculated a dispersivity value of 12.5 m without the assumption of layers; our calculation of 10.5 m is in close agreement. Our calculations indicate that dispersivity increases with scale, accounting for nonuniform flow effects and without the arbitrary assumption of geologic layers.

Savannah River Plant, Georgia.   Webster et al. [1970] evaluated data from a two-well recirculating test using the methodology of Grove and Beetem [1971]. This analysis assumes uniform flow along stream tubes and sums individual breakthrough curves along the stream tubes to obtain a composite breakthrough curve. A dispersivity value of 134 m at a scale of 538 m was obtained using this method. We reevaluated the data using the methodology of Gelhar [1982] which accounts for nonuniform flow effects. We obtained a dispersivity value of 47 m from our analysis. We have more confidence in this value because the analysis more accurately represents the actual flow configuration.

Tucson, Arizona.   The data reported by Wilson [1971] for a two-well test were also evaluated by Robson [1974] using a Grove and Beetem–type analysis. Wilson reported a value of longitudinal dispersivity of 15.2 m at a scale of 79.2 m. Using a nonuniform flow solution based on that of Gelhar [1982], we calculated a value of longitudinal dispersivity of 1.2 m, an order of magnitude smaller than that of Robson. Again, we have more confidence in this value because the analysis more accurately reflects the actual flow situation.

Columbus, Mississippi.   The natural gradient tracer test at the Columbus site (E. E. Adams and L. W. Gelhar, Field
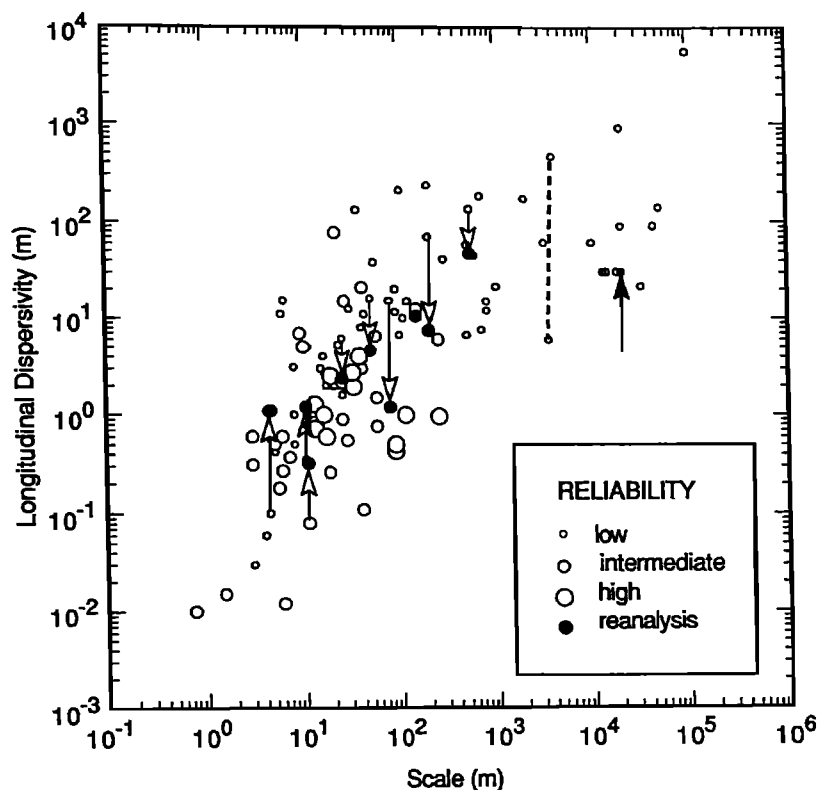
Fig. 3. Longitudinal dispersivity versus scale of observation with adjustments resulting from reanalyses. Arrows indicate reported values at tails and corresponding values from reanalyses at heads. Dashed line connects two dispersivity values determined at the Hanford site.

study of dispersion in a heterogeneous aquifer: Spatial moments analysis, submitted to *Water Resources Research*, 1991; hereinafter Adams and Gelhar, submitted manuscript, 1991) is unique in that the large-scale ambient flow field exhibits strong nonuniformity and the aquifer is very heterogeneous. A superficial spatial moments interpretation, ignoring the flow nonuniformity, indicated a longitudinal dispersivity of around 70 m, whereas a more refined analysis that explicitly includes the influence of flow nonuniformity yields a dispersivity of around 7 m (Adams and Gelhar, submitted manuscript, 1991). This refined estimate is regarded to be of intermediate reliability because of the uncertainty regarding the mass balance at the Columbus site.

From the above reanalyses, all values of dispersivity calculated were smaller than the original values. We have higher confidence in these values because they are associated with solutions to the advection-dispersion equation with more realistic assumptions. In all cases we would rate the new values to be of intermediate reliability instead of low reliability. The reevaluated data are shown as solid symbols on Figure 3 connected to their original values by vertical arrows.

Based on the above reanalyses, we suspect that it is most likely that improved analyses would reduce many of the lower-reliability dispersivities in Figure 2. However, there are a few cases for which more appropriate observations and/or interpretations would most likely lead to larger dispersivities. For example, the Twin Lake natural gradient tracer test [*Moltyaner and Killey*, 1988a, b] was interpreted by using breakthrough curves at individual boreholes con-

structed as the average of breakthrough curves in three somewhat arbitrarily defined layers. We suspect that this kind of localized observation will produce a significantly lower dispersivity than would result from a spatial moments analysis which considers the overall spreading of the plume. The magnitude of the possible increase in the dispersivity cannot be assessed because the sampling network did not completely encompass the plume at the Twin Lake site.

Another example is that of the first Borden site natural gradient experiment [*Sudicky et al.*, 1983] which was analyzed using an analytical solution with spatially constant dispersivities. In the near-source region where dispersivities are actually increasing with displacement, this approach will tend to underestimate the magnitude of the dispersivity. *Gelhar et al.* [1985] reanalyzed the first Borden experiment using the method of spatial moments and found that the longitudinal dispersivity at 11 m was 2–4 times that found by *Sudicky et al.* [1983]. The resulting increase in the dispersivity is illustrated in Figure 3 connected to the original point by a vertical line. Because of the incomplete plume sampling and plume bifurcation in this test (only the "slow zone" was analyzed), this point is still regarded to be of intermediate reliability.

Dispersivities at small displacements will also be underestimated if based on breakthrough curves measured in localized samplers in individual layers. Such effects are likely, for example, in the Perch Lake [*Lee et al.*, 1980] and Lower Glatt Valley [*Hoehn*, 1983] interpretations. Later interpretation of the Lower Glatt Valley data using temporal moments [*Hoehn and Santschi*, 1987] shows values an order of

magnitude larger; these are connected with the original values by vertical lines in Figure 3.

As a further illustration of the uncertainty in the longitudinal dispersivity values in Figure 2, consider the data for the Hanford site. The tracer test [*Bierschenk*, 1959; *Cole*, 1972] interpreted from breakthrough curves at two different wells at roughly the same distance (around 4000 m) from the injection point produced values differing by 2 orders of magnitude (see dashed line in Figure 3). This difference illustrates the difficulty in interpreting point breakthrough curves in heterogeneous aquifers, even at this large displacement. The numerical simulations of the contamination plume [*Ahlstrom et al.*, 1977] extending to 20,000 m used a dispersivity of 30.5 m (100 feet) as identified by the bold arrow in Figure 3. Evidently this round number (100 feet) was popular in several different simulations of contaminant plumes.

In none of the cases of simulations of contamination events is there any explicit information on how the dispersivity values were selected or in what sense the values may be optimal. Consequently it is not possible to quantify the uncertainty in dispersivity values based on contamination event simulations. However, experience suggests that, because of the possible tendency to select large dispersivities which avoid the numerical difficulties associated with large grid Peclet numbers, some of the dispersivity values based on contaminant plumes are likely to be biased toward higher values. Such overestimates would occur mainly at larger scales.
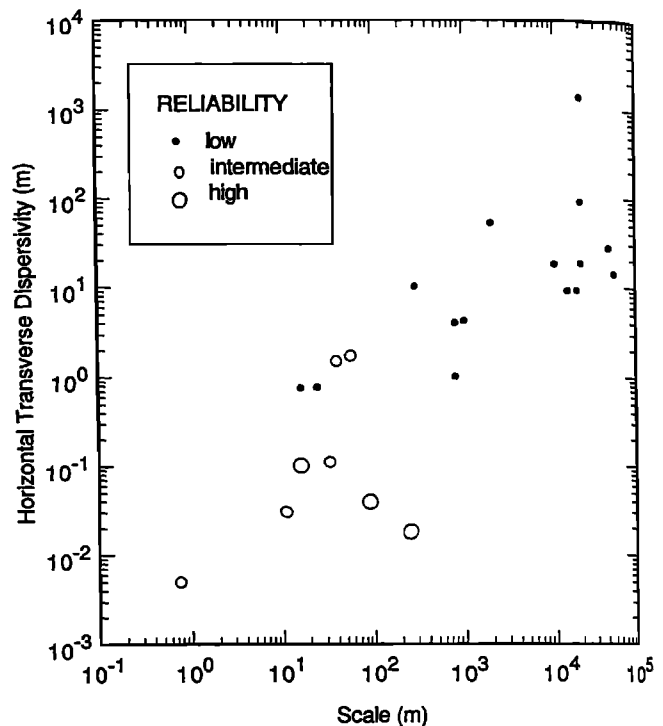
The results of these reanalyses provide an explicit indication of the uncertainty in the dispersivity values in Figure 2 and suggest that for large displacements the low-reliability dispersivities are likely to decrease whereas for small displacements some increases can be expected.

Transverse Dispersivities

Although the data on transverse dispersivity are much more limited, they reveal some features which are important in applications. The data on horizontal and vertical transverse dispersivities are summarized in Figures 4 and 5, which show these parameters as a function of scale of observation. The data are portrayed in terms of reliability classification with the largest symbols identifying the high-reliability points.

In the case of the horizontal dispersivity, there appears to be some trend of increasing dispersivity with scale but this appearance results from low-reliability data which finds their origin largely in contaminant event simulations using two-dimensional depth-averaged descriptions. In these contamination situations the sources are often ill-defined; if the actual source area is larger than that represented in the model there will be greater transverse spreading which would incorrectly be attributed to transverse dispersion.

In the case of vertical transverse dispersion (Figure 5), the data are even more limited and certainly do not imply any significant trend with overall scale. Note that there are only two points of high reliability, those corresponding to the Borden [*Freyberg*, 1986] and Cape Cod [*Garabedian et al.*, 1988, 1991] sites. The estimate of the vertical transverse dispersivity for the Borden site is from the recent three-dimensional analysis of *Rajaram and Gelhar* [1991]. The vertical transverse dispersivity is seen to be much smaller than the horizontal transverse dispersivity, apparently reflecting the roughly horizontal stratification of hydraulic conductivity encountered in permeable sedimentary materi-
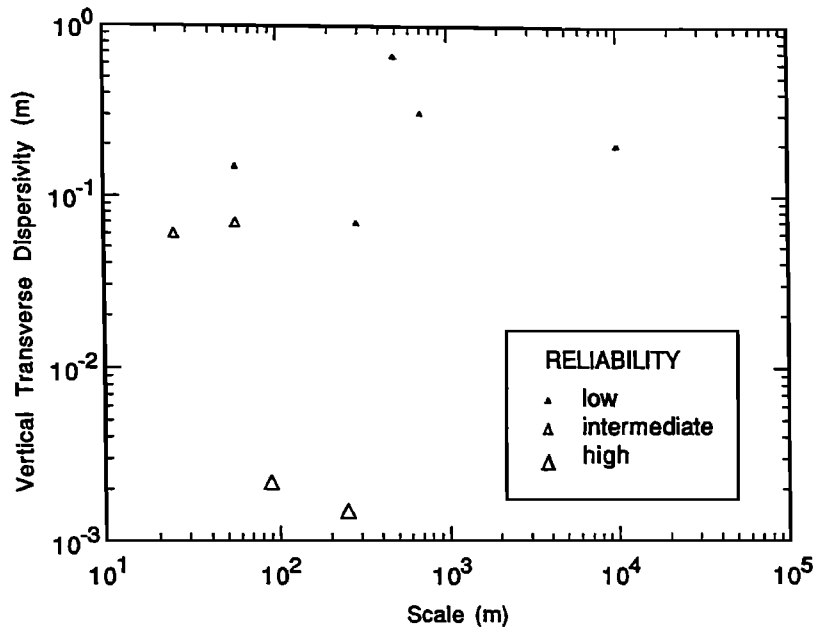

Fig. 4. Horizontal transverse dispersivity as a function of observation scale.

als. All of the vertical dispersivities are less than 1 m and high-reliability values are only a few millimeters, this being the same order of magnitude as the local transverse dispersivity for sandy materials.

The ratio of longitudinal dispersivity to the horizontal and vertical transverse dispersivities is shown in Figure 6. This form of presentation is used because it is common practice to select constant values for the ratio of longitudinal to transverse dispersivities. For one thing, this plot illustrates the popularity of using, in numerical simulations, a horizontal transverse dispersivity which is about one third of the longitudinal dispersivity (the horizontal dashed line in Figure 6). There does not appear to be any real justification for using this ratio. We are not aware of any simulation work which systematically demonstrates the appropriateness of this value for the horizontal transverse dispersivity. The two high-reliability points show an order of magnitude higher ratio of longitudinal to horizontal transverse dispersivities. The vertical dashed lines in Figure 6 are used to identify three-dimensionally monitored sites for which all three principal components of the dispersivity tensor have been estimated. In all of these cases, the vertical transverse dispersivity is 1–2 orders of magnitude smaller than the horizontal transverse dispersivity. This behavior further emphasizes the small degree of vertical mixing which is frequently encountered in naturally stratified sediments. This small degree of vertical mixing is clearly an important consideration in many applications, such as the design of observation networks to monitor contamination plumes and the development of remediation schemes. Consequently, in order to model many field situations realistically, it will be necessary to use three-dimensional transport models which adequately represent the small but finite vertical mixing.

Fig. 5. Vertical transverse dispersivity as a function of observation scale.

INTERPRETATIONS

This review of field observations of dispersive mixing in aquifers demonstrates several overall features which are evident from the graphical and tabular information developed here. Taken in aggregate, without regard for reliability, the data indicate a clear trend of systematic increase of longitudinal dispersivity with scale. In terms of aquifer type (porous versus fractured media) the data at smaller scale may seem to be higher for fractured media but, in view of the lower reliability of the fractured media data, this difference is of minimal significance.

When the data on longitudinal dispersivity are classified according to reliability, the pattern regarding scale dependence of dispersivity is less clear (see Figure 2). There are no high-reliability points at scales greater than 300 m and the high-reliability points are systematically in the lower portion of the scattering of data. The lack of high-reliability data at scales greater than 300 m reflects the fact that the data beyond that scale are almost exclusively from contamination simulations or environmental tracer studies for which the solute input is typically ill-defined. Because of the very long period of time required to carry out controlled input tracer experiments at these larger scales, such experiments have not been undertaken.

Although the data shown in Figure 2 suggest that some overall trend of increasing dispersivity with scale is plausible, it does not seem reasonable to conclude that a single universal line [Neuman, 1990] can be meaningfully identified
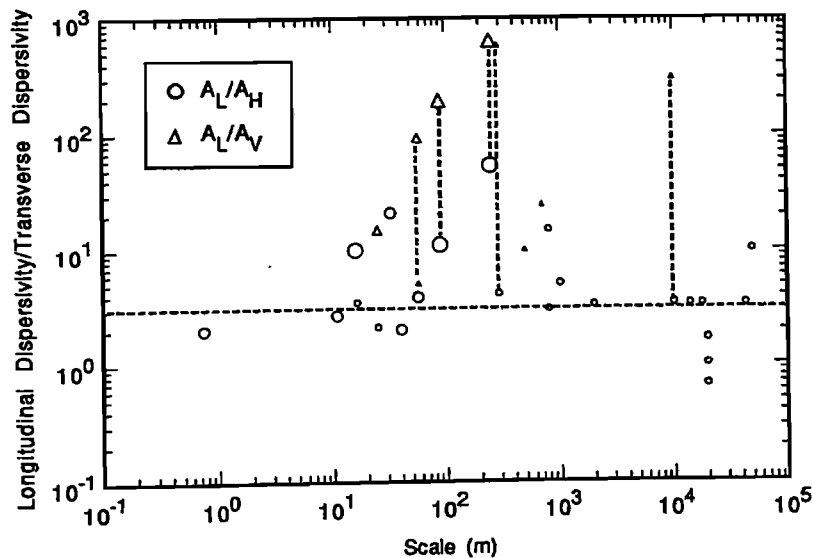
Fig. 6. Ratio of longitudinal to horizontal and vertical transverse dispersivities; largest symbols are high reliability and smallest symbols are low reliability. Vertical dashed lines connecting two points indicate sites where all three principal components of the dispersivity tensor have been measured. Horizontal dashed line indicates a ratio of A_L/A_T = 1/3, which has been widely used in numerical simulations.

by applying standard linear regression to all of the data. Rather we would expect a family of curves reflecting different dispersivities in aquifers with different degrees of heterogeneity. At a given scale, the longitudinal dispersivity typically ranges over 2–3 orders of magnitude. This degree of variation can be explained in terms of the established stochastic theory [e.g., *Gelhar and Axness*, 1983; *Dagan*, 1984] which shows that the longitudinal dispersivity is proportional to the product of the variance and the correlation scale of the natural logarithm of hydraulic conductivity. A compilation of data on these parameters [*Gelhar*, 1986] shows that they vary over a range that can easily explain the range of variation in Figure 2. The theoretical results for the developing dispersion process [*Gelhar et al.*, 1979; *Dagan*, 1984; *Gelhar*, 1987; *Naff et al.*, 1988] show that the longitudinal dispersivity initially increases linearly with displacement distance and gradually approaches a constant asymptotic value [see *Gelhar*, 1987, Figure 9]. One could visualize the behavior of Figure 2 as being the result of superimposing several such theoretical curves with different parameters characterizing aquifer heterogeneity.

The results of reanalyses for several of the individual sites serve to illustrate explicitly the uncertainty involved in the estimates of longitudinal dispersivity. The reanalyses indicate that, for the most part, improved analysis will lead to decreases in the longitudinal dispersivity except possibly for very small displacements where limited localized sampling can produce underestimates of the bulk spreading and mixing. In cases where the dispersivity estimates were based on numerical simulations of contamination events, the degree of uncertainty is likely large and ill-determined, but bias in some of the estimates toward the high side seems most likely.

From an applications perspective, the information assembled here should serve as a strong cautionary note about routinely adopting dispersivities from Figure 2 or a linear regression representation through the data. We feel that the preponderance of evidence favors the use of dispersivity values in the lower half of the range at any given scale. If values in the upper part of the range are adopted, excessively large dilution may be predicted and the environmental consequences misrepresented. In the case of transverse dispersivities, it is particularly important to recognize the very low vertical transverse dispersivities that have been observed at several sites. As a result, many contamination plumes will exhibit very limited vertical mixing with high concentrations at a given horizon. The recognition of such features is of obvious importance in designing monitoring schemes and implementing aquifer remediation. Horizontal transverse dispersivities are typically an order of magnitude smaller than the longitudinal dispersivity whereas vertical transverse dispersivities are another order of magnitude lower.

From a research perspective, the data reviewed here suggest a need for some skepticism regarding "universal" models which represent the scattered data of varying reliability by a single straight line. The presumption of such a universal model ignores the fact that different aquifers will have different degrees of heterogeneity at a given scale. The data suggest that there is a scale dependence of longitudinal dispersivity but reliable data must be developed at larger scales in order to establish the nature of the dependence. Clearly, there is a need for very large scale, long-term, carefully planned experiments extending to several kilometers.

REFERENCES

Ahlstrom, S. W., H. P. Foote, R. C. Arnett, C. P. Cole, and R. J. Serne, Multicomponent mass transport model: Theory and numerical implementation (discrete-particle-random-walk-version), *Rep. BNWL-2127*, Battelle Pac. Northwest Lab., Richland, Wash., 1977.

Anderson, M. P., Using models to simulate the movement of contaminants through groundwater flow systems, *CRC Crit. Rev. Environ. Control*, 9, 97–156, 1979.

Bassett, R. L., et al., Preliminary data from a series of artificial recharge experiments at Stanton, Texas, *U.S. Geol. Surv. Open File Rep., 81-0149*, 1980.

Bear, J., *Dynamics of Fluids in Porous Media*, Elsevier Scientific, New York, 1972. (Reprinted by Dover, New York, 1988.)

Beims, U., Planung, Durchführung und Auswertung von Gütepumpversuchen, *Z. Angew. Geol.*, 29(10), 482–490, 1983.

Bentley, H. W., and G. R. Walter, Two-well recirculating tracer tests at H-2: Waste Isolation Pilot Plant (WIPP), southwest New Mexico, draft paper, Hydro Geochem., Inc., Tucson, Ariz., 1983.

Betson, R. P., J. M. Boggs, S. C. Young, W. R. Waldrop, and L. W. Gelhar, Macrodispersion experiment (MADE): Design of a field experiment to investigate transport processes in a saturated groundwater zone, *Rep. EPRI EA-4082*, Elec. Power Res. Inst., Palo Alto, Calif., June 1985.

Bierschenk, W. H., Aquifer characteristics and ground-water movement at Hanford, *Rep. HW-60601*, Hanford At. Products Oper., Richland, Wash., 1959.

Bredehoeft, J. D., and G. F. Pinder, Mass transport in flowing groundwater, *Water Resour. Res.*, 9(1), 144–210, 1973.

Claasen, H. C., and E. H. Cordes, Two-well recirculating tracer test in fractured carbonate rock, Nevada, *Hydrol. Sci. Bull..*, 20(3), 367–382, 1975.

Cole, J. A., Some interpretations of dispersion measurements in aquifers, *Groundwater Pollution in Europe*, edited by J. A. Cole, pp. 86–95, Water Research Association, Reading, England, 1972.

Dagan, G., Stochastic modeling of groundwater flow by unconditional and conditional probabilities, 2, The solute transport, *Water Resour. Res.*, 18(4), 835–848, 1982.

Dagan, G., Solute transport in heterogeneous porous formations, *J. Fluid Mech.*, 145, 151–177, 1984.

Daniels, W. R. (Ed.), Laboratory field studies related to the radionuclide migration project, *Progress Rep. LA-8670-PR*, Los Alamos Sci. Lab., Los Alamos, N. M., 1981.

Daniels, W. R. (Ed.), Laboratory field studies related to the radionuclide migration project (draft), *Progress Rep. LA-9192-PR*, Los Alamos Sci. Lab., Los Alamos, N. M., 1982.

Davis, S. N., G. M. Thompson, H. W. Bentley, and G. Stiles, Groundwater tracers—A short review, *Ground Water*, 18(1), 14–23, 1980.

Davis, S. N., D. J. Campbell, H. W. Bentley, and T. J. Flynn, An introduction to groundwater tracers, *Rep. EPA/600/2-85/022*, Environ. Prot. Agency, Washington, D. C., 1985. (Available as *NTIS PB86-100591* from Natl. Tech. Inf. Serv., Springfield, Va.)

de Marsily, G., *Quantitative Hydrogeology*, Academic, San Diego, Calif., 1986.

Dieulin, A., Propagation de pollution dans un aquifere alluvial: L'effet de parcours, doctoral dissertation, Univ. Pierre et Marie Curie-Paris VI and l'Ecole Natl. Super. des Mines de Paris, Fontainebleau, France, 1980.

Dieulin, A., Lixiviation in situ d'un gisement d'uranium en milieu granitique, *Draft Rep. LHM/RD/81/63*, Ecole Natl. Super. des Mines de Paris, Fontainebleau, France, 1981.

Egboka, B. C. E., J. A. Cherry, R. N. Farvolden, and E. O. Frind, Migration of contaminants in groundwater at a landfill: A case study, 3, Tritium as an indicator of dispersion and recharge, *J. Hydrol.*, 63, 51–80, 1983.

Fenske, P. R., Hydrology and radionuclide transport, monitoring well HT-2m, Tatum Dome, Mississippi, *Proj. Rep. 25, Tech. Rep.*

NVD-1253-6, Cent. for Water Resour. Res., Desert Res. Inst., Univ. of Nev. Syst., Reno, 1973.

Freyberg, D. L., A natural gradient experiment on solute transport in a sand aquifer, 2, Spatial moments and the advection and dispersion of nonreactive tracers, Water Resour. Res., 22(13), 2031–2046, 1986.

Fried, J. J., Groundwater Pollution, Elsevier, New York, 1975.

Fried, J. J., and P. Ungemach, Determination in situ du coefficient de dispersion longitudinale d'un milieu poreux naturel, C. R. Acad. Sci., Ser. 2, 272, 1327–1329, 1971.

Garabedian, S. P., L. W. Gelhar, and M. A. Celia, Large-scale dispersive transport in aquifers: Field experiments and reactive transport theory, Rep. 315, Ralph M. Parsons Lab. for Water Resour. and Hydrodyn., Mass. Inst. of Technol., Cambridge, 1988.

Garabedian, S. P., D. R. LeBlanc, L. W. Gelhar, and M. A. Celia, Large-scale natural gradient tracer test in sand and gravel, Cape Cod, Massachusetts, 2, Analysis of tracer moments for a nonreactive tracer, Water Resour. Res., 27(5), 911–924, 1991.

Gelhar, L. W., Analysis of two-well tracer tests with a pulse input, Rep. RHO-BW-CR-131 P, Rockwell Intl., Richland, Wash., 1982.

Gelhar, L. W., Stochastic subsurface hydrology from theory to applications, Water Resour. Res., 22, 135S–145S, 1986.

Gelhar, L. W., Stochastic analysis of solute transport in saturated and unsaturated porous media, NATO ASI Ser., Ser. E, 128, 657–700, 1987.

Gelhar, L. W., and C. L. Axness, Three dimensional stochastic analysis of macrodispersion in aquifers, Water Resour. Res., 19(1), 161–180, 1983.

Gelhar, L. W., A. L. Gutjahr, and R. L. Naff, Stochastic analysis of macrodispersion in a stratified aquifer, Water Resour. Res., 15(6), 1387–1397, 1979.

Gelhar, L. W., A. Mantaglou, C. Welty, and K. R. Rehfeldt, A review of field-scale physical solute transport processes in saturated and unsaturated porous media, EPRI Rep. EA-4190, Elec. Power Res. Inst., Palo Alto, Calif., Aug. 1985.

Goblet, P., Interpretation d'experiences de tracage en milieu granitique (site B), Rep. LHM/RD/82/11, Cent. d'Inf. Geol., Ecole Natl. Super. des Mines de Paris, Fontainebleau, France, 1982.

Grove, D. B., The use of Galerkin finite-element methods to solve mass transport equations, Rep. USGS/WRD/WRI-78/011, U.S. Geol. Surv., Denver, Colo., 1977. (Available as NTIS PB 277-532 from Natl. Tech. Inf. Serv., Springfield, Va.)

Grove, D. B., and W. A. Beetem, Porosity and dispersion constant calculations for a fractured carbonate aquifer using the two-well tracer method, Water Resour. Res., 7(1), 128–134, 1971.

Gupta, S. K., K. K. Tanji, and J. N. Luthin, A three-dimensional finite element ground water model, Rep. UCAL-WRC-C-152, Calif. Water Resour. Cent., Univ. of Calif., Davis, 1975. (Available as NTIS PB 248-925 from Natl. Tech. Inf. Serv., Springfield, Va.)

Halevy, E., and A. Nir, Determination of aquifer parameters with the aid of radioactive tracers, J. Geophys. Res., 67(5), 2403–2409, 1962.

Harpaz, Y., Field experiments in recharge and mixing through wells, Underground Water Storage Study Tech. Rep. 17, Publ. 483, Tahal–Water Plann. for Isr., Tel Aviv, 1965.

Heller, J. P., Observations of mixing and diffusion in porous media, Proc. Symp. Fundam. Transp. Phenom. Porous Media, 2nd, 1–26, 1972.

Helweg, O. J., and J. W. Labadie, Linked models for managing river basin salt balance, Water Resour. Res., 13(2), 329–336, 1977.

Hoehn, E., Geological interpretation of local-scale tracer observations in a river-ground water infiltration system, draft report, Swiss Fed. Inst. Reactor Res. (EIR), Würenlingen, Switzerland, 1983.

Hoehn, E., and P. H. Santschi, Interpretation of tracer displacement during infiltration of river water to groundwater, Water Resour. Res., 23(4), 633–640, 1987.

Huyakorn, P. S., P. F. Anderson, F. J. Motz, O. Güven, and J. G. Melville, Simulations of two-well tracer tests in stratified aquifers at the Chalk River and the Mobile sites, Water Resour. Res., 22(7), 1016–1030, 1986.

Iris, P., Contribution à l'étude de la valorisation energetique des aquifères peu profonds, thèse de docteur-ingenieur, Ecole des Mines de Paris, Fontainebleau, France, 1980.

Ivanovitch, M., and D. B. Smith, Determination of aquifer parameters by a two-well pulsed method using radioactive tracers, J. Hydrol., 36(1/2), 35–45, 1978.

Kies, B., Solute transport in unsaturated field soil and in groundwater, Ph.D. dissertation, Dep. of Agron., N. M., State Univ., Las Cruces, 1981.

Klotz, D., K. P. Seiler, H. Moser, and F. Neumaier, Dispersivity and velocity relationship from laboratory and field experiments, J. Hydrol., 45(3/4), 169–184, 1980.

Konikow, L. F., Modeling solute transport in ground water, in Environmental Sensing and Assessment: Proceedings of the International Conference, article 20-3, Institute for Electrical and Electronic Engineers, Piscataway, N. J., 1976.

Konikow, L. F., and J. D. Bredehoeft, Modeling flow and chemical quality changes in an irrigated stream-aquifer system, Water Resour. Res., 10(3), 546–562, 1974.

Kreft, A., A. Lenda, B. Turek, A. Zuber, and K. Czauderna, Determination of effective porosities by the two-well pulse method, Isot. Tech. Groundwater Hydrol., Proc. Symp., 2, 295–312, 1974.

Lallemande-Barres, A., and P. Peaudecerf, Recherche des relations entre la valeur de la dispersivité macroscopique d'un milieu aquifère, ses autres caractéristiques et les conditions de mesure, Bull. Bur. Rech. Geol. Min., Sect. 3, Ser. 2, 4, 1978.

Lau, L. K., W. J. Kaufman, and D. K. Todd, Studies of dispersion in a radial flow system, Canal Seepage Research: Dispersion Phenomena in Flow Through Porous Media, Progress Rep. 3, I.E.R. Ser. 93, Issue 3, Sanit. Eng. Res. Lab., Dep. of Eng. and School of Public Health, Univ. of Calif., Berkeley, 1957.

LeBlanc, D. R., Sewage plume in a sand and gravel aquifer, Cape Cod, Massachusetts, U.S. Geol. Surv. Open File Rep., 82-274, 35 pp., 1982.

Lee, D. R., J. A. Cherry, and J. F. Pickens, Groundwater transport of a salt tracer through a sandy lakebed, Limnol. Oceanogr., 25(1), 46–61, 1980.

Leland, D. F., and D. Hillel, Scale effects on measurement of dispersivity in a shallow, unconfined aquifer, paper presented at Chapman Conference on Spatial Variability in Hydrologic Modeling, AGU, Fort Collins, Colo., July 21–23, 1981.

Lenda, A., and A. Zuber, Tracer dispersion in groundwater experiments, in Isot. Hydrol. Proc. Symp. 1970, 619–641, 1970.

MacFarlane, D. S., J. A. Cherry, R. W. Gilham, and E. A. Sudicky, Migration of contaminants at a landfill: A case study, 1, Groundwater flow and plume delineation, J. Hydrol., 63, 1–29, 1983.

Mercado, A., Recharge and mixing tests at Yavne 20 well field, Underground Water Storage Study Tech. Rep. 12, Publ. 611, Tahal–Water Plann. for Isr., Tel Aviv, 1966.

Meyer, B. R., C. A. R. Bain, A. S. M. DeJesus, and D. Stephenson, Radiotracer evaluation of groundwater dispersion in a multilayered aquifer, J. Hydrol., 50(1/3), 259–271, 1981.

Molinari, J., and P. Peaudecerf, Essais conjoints en laboratoire et sur le terrain en vue d'une approach simplefiée de la prévision des propagations de substances miscibles dans les aquifères réels, paper presented at Symposium on Hydrodynamic Diffusion and Dispersion in Porous Media, Int. Assoc. for Hydraul. Res., Pavis, Italy, 1977.

Moltyaner, G. L., and R. W. D. Killey, Twin Lake tracer tests: Longitudinal dispersion, Water Resour. Res., 24(10), 1613–1627, 1988a.

Moltyaner, G. L., and R. W. D. Killey, Twin Lake tracer tests: Transverse dispersion, Water Resour. Res., 24(10), 1628–1637, 1988b.

Molz, F. J., O. Güven, and J. G. Melville, An examination of scale-dependent dispersion coefficients, Ground Water, 21, 715–725, 1983.

Molz, F. J., O. Güven, J. G. Melville, R. D. Crocker, and K. T. Matteson, Performance, analysis, and simulation of a two-well tracer test at the Mobile site, Water Resour. Res., 22(7), 1031–1037, 1986.

Naff, R. L., T.-C. J. Yeh, and M. W. Kemblowski, A note on the recent natural gradient tracer test at the Borden site, Water Resour. Res., 24(12), 2099–2103, 1988.

Naymik, T. G., and M. J. Barcelona, Characterization of a contaminant plume in ground water, Meredosia, Illinois, Ground Water, 19(5), 517–526, 1981.

Neretnieks, I., Transport in fractured rocks, paper presented at the

17th International Congress on the Hydrology of Rock of Low Permeability, Intl. Assoc. of Hydrogeol., Tucson, Ariz., Jan. 7-12, 1985.

Neuman, S. P., Universal scaling of hydraulic conductivities in geologic media, Water Resour. Res., 26(8), 1749-1758, 1990.

Neuman, S. P., C. L. Winter, and C. M. Newman, Stochastic theory of field-scale dispersion in anisotropic porous media, Water Resour. Res., 23(3), 453-466, 1987.

New Zealand Ministry of Works and Development, Water and Soil Division, Movement of contaminants into and through the Heretaunga Plains aquifer, report, Wellington, 1977.

Oakes, D. B., and D. J. Edworthy, Field measurement of dispersion coefficients in the United Kingdom, in Ground Water Quality, Measurement, Prediction, and Protection, pp. 327-340, Water Research Centre, Reading, England, 1977.

Papadopulos, S. S., and S. P. Larson, Aquifer storage of heated water: II, Numerical simulation of field results, Ground Water, 16(4), 242-248, 1978.

Perlmutter, N. M., and M. Lieber, Dispersal of plating wastes and sewage contaminants in the groundwater and surface water: South Farmingdale-Massapequid area, Nassau County, New York, U.S. Geol. Surv. Water Supply Pap., 1879-G, 1970.

Philip, J. R., Issues in flow and transport in heterogeneous porous media, Transp. Porous Media, 1, 319-338, 1986.

Pickens, J. F., and G. E. Grisak, Scale dependent dispersion in a stratified granular aquifer, Water Resour. Res., 17(4), 1191-1211, 1981.

Pinder, G. F., A Galerkin-finite element simulation of groundwater contamination on Long Island, Water Resour. Res., 9(6), 1657-1669, 1973.

Rabinowitz, D. D., and G. W. Gross, Environmental tritium as a hydrometeorologic tool in the Roswell Basin, New Mexico, Tech. Completion Rep. OWRR:A-037-NMEX, N. M. Water Resour. Res. Inst., Las Cruces, 1972.

Rajaram, H., and L. W. Gelhar, Three-dimensional spatial moments analysis of the Borden tracer test, Water Resour. Res., 27(6), 1239-1251, 1991.

Roberts, P. V., M. Reinhard, G. D. Hopkins, and R. S. Summers, Advection-dispersion-sorption models for simulating the transport of organic contaminants, paper presented at International Conference on Ground Water Quality Research, Rice Univ., Houston, Tex., 1981.

Robertson, J. B., Digital modeling of radioactive and chemical waste transport in the Snake River Plain aquifer of the National Reactor Testing Station, Idaho, U.S. Geol. Surv. Open File Rep., IDO-22054, 1974.

Robertson, J. B., and J. T. Barraclough, Radioactive and chemical waste transport in groundwater of National Reactor Testing Station: 20-year case history and digital model, Underground Waste Manage. Artif. Recharge Prepr. Pap. Int. Symp. 2nd, 1, 291-322, 1973.

Robson, S. G., Feasibility of digital water quality modeling illustrated by application at Barstow, California, U.S. Geol. Surv. Water Resour. Invest., 46-73, 1974.

Robson, S. G., Application of digital profile modeling techniques to ground-water solute transport at Barstow, California, U.S. Geol. Surv. Water Supply Pap., 2050, 1978.

Rousselot, D., J. P. Sauty, and B. Gaillard, Etude hydrogéologique de la zone industrielle de Blyes-Saint-Vulbas, rapport préliminaire no. 5: Caracteristiques hydrodynamiques du système aquifère, Rep. Jal 77/33, Bur. de Rech. Geol. et Min., Orleans, France, 1977.

Sauty, J. P., Contribution à l'identification des paramèters de dispersion dans les aquifères par interprétation des expériences de tracage, dissertation, Univ. Sci. et Med. et Inst. Natl. Polytech. de Grenoble, Grenoble, France, 1977.

Sauty, J. P., An analysis of hydrodispersive transfer in aquifers, Water Resour. Res., 16(1), 145-158, 1980.

Sauty, J. P., A. C. Gringarten, and P. A. Landel, The effects of thermal dispersion on injection of hot water in aquifers, paper presented at Invitational Well-Testing Symposium, Lawrence Berkeley Lab., Berkeley, Calif., 1978.

Segol, G., and G. F. Pinder, Transient simulation of saltwater intrusion in southeastern Florida, Water Resour. Res., 12(1), 65-70, 1976.

Sudicky, E. A., J. A. Cherry, and E. O. Frind, Migration of contaminants in groundwater at a landfill: A case study, 4, A natural-gradient dispersion test, J. Hydrol., 63, 81-108, 1983.

Sykes, J. F., S. B. Pahwa, R. B. Lantz, and D. S. Ward, Numerical simulation of flow and contaminant migration at an extensively monitored landfill, Water Resour. Res., 18(6), 1687-1704, 1982.

Sykes, J. F., S. B. Pahwa, D. S. Ward, and D. S. Lantz, The validation of SWENT, a geosphere transport model, in Scientific Computing, edited by R. Stapleman et al., pp. 351-361, IMAES/North-Holland, Amsterdam, 1983.

Vaccaro, J. J., and E. L. Bolke, Evaluation of water quality characteristics of part of the Spokane aquifer, Washington and Idaho, using a solute transport digital model, U.S. Geol. Surv. Open File Rep., 82-769, 1983.

Valocchi, A. J., P. V. Roberts, G. A. Parks, and R. L. Street, Simulation of the transport of ion-exchanging solutes using laboratory-determined chemical parameter values, Ground Water, 19(6), 600-607, 1981.

Walter, G. B., Convergent flow tracer test at H-6: Waste isolation pilot plant (WIPP), southeast New Mexico (draft), Hydro Geochem, Inc., Tucson, Ariz., 1983.

Webster, D. S., J. F. Procter, and J. W. Marine, Two-well tracer test in fractured crystalline rock, U.S. Geol. Surv., Water Supply Pap., 1544-I, 1970.

Welty, C., and L. W. Gelhar, Evaluation of longitudinal dispersivity from tracer test data, Rep. 320, Ralph M. Parsons Lab. for Water Resour. and Hydrodyn., Mass. Inst. of Technol., Cambridge, 1989.

Werner, A., et al., Nutzung von Grundwasser fur Warmepumpen, Versickerrungstest Aefligen, Versuch 2, 1982/83, Water and Energy Manage. Agency of the State of Bern, Switzerland, 1983.

Wheatcraft, S. W., and S. W. Tyler, An explanation of scale-dependent dispersivity in heterogeneous aquifers using concepts of fractal geometry, Water Resour. Res., 24(4), 566-578, 1988.

Wiebenga, W. A., et al., Radioisotopes as groundwater tracers, J. Geophys. Res., 72(16), 4081-4091, 1967.

Wilson, L. G., Investigations on the subsurface disposal of waste effluents at inland sites, Res. Develop. Progress Rep. 650, U.S. Dep. of Interior, Washington, D. C., 1971.

Wood, W., A geochemical method of determining dispersivity in regional groundwater systems, J. Hydrol., 54(1/3), 209-224, 1981.

Wood, W. W., and G. G. Ehrlich, Use of baker's yeast to trace microbial movement in ground water, Ground Water, 16(6), 398-403, 1978.

L. W. Gelhar, Ralph M. Parsons Laboratory, Department of Civil Engineering, Massachusetts Institute of Technology, Cambridge, MA 02139.

K. R. Rehfeldt, Illinois State Water Survey, 2204 Griffith Drive, Champaign, IL 61820.

C. Welty, Department of Civil and Architectural Engineering, Drexel University, Philadelphia, PA 19104.